AFOSR TR 97-0716

REPORT DOCUMENTATION PAGE

Public reporting burden for this collection of information is estimated to average 1 hour per response, including the time for reviewing instructions, searching existing data sources, gathering and maintaining the data needed, and completing and reviewing the collection of information. Send comments regarding this burden estimate or any other aspect of this collection of information, including suggestions for reducing this burden, to Washington Headquarters Services, Directorate for Information Operations and Reports, 1215 Jefferson Davis Highway, Suite 1204, Arlington, VA 22202-4302, and to the Office of Management and Budget, Paperwork Reduction Project (0704-0188), Washington, DC 20503.

1. AGENCY USE ONLY (Leave blank)	2. REPORT DATE	3. REPORT TYPE AND DATES COVERED
		FINAL 01 May 94 to 30 Apr 98

4. TITLE AND SUBTITLE
ABSORPTION BACKSCATTERING AND MIRROR REFLECTION FROM LASER AND MICROWAVE PRODUCED PLASMAS

5. FUNDING NUMBERS
61102F
2301/ES

6. AUTHOR(S)
PROFESSOR SCHARER

7. PERFORMING ORGANIZATION NAME(S) AND ADDRESS(ES)
UNIVERSITY OF WISCONSIN
750 UNIVERSITY AVENUE
MADISON WI 53706

8. PERFORMING ORGANIZATION REPORT NUMBER

9. SPONSORING/MONITORING AGENCY NAME(S) AND ADDRESS(ES)
AFOSR/NE
110 DUNCAN AVE ROOM B115
BOLLING AFB DC 20332-8050

10. SPONSORING/MONITORING AGENCY REPORT NUMBER
F49620-94-1-0054

11. SUPPLEMENTARY NOTES

12a. DISTRIBUTION/AVAILABILITY STATEMENT
APPROVAL FOR PUBLIC RELEASE: DISTRIBUTION UNLIMITED

12b. DISTRIBUTION CODE

13. ABSTRACT (Maximum 200 words)

Research on an improved 8-10 GHz microwave system for propagation, reflection and absorption studies of VUV excimer laser (193 nm) produced plasmas has been carrier out. We have obtained high density ne =2-5x10 13/cm3 laser-formed plasmas which are 9cm wide x 40cm long x 3-20 mm thick and demonstrated that diffusion is small for time scales less than a microsceond. Preliminary results show that the initial high density plasma obtained in TMAE at 30-60 m Torr pressures has a reflection coefficient comparable to aluminum.

19971217 074

14. SUBJECT TERMS			15. NUMBER OF PAGES
			16. PRICE CODE

17. SECURITY CLASSIFICATION OF REPORT	18. SECURITY CLASSIFICATION OF THIS PAGE	19. SECURITY CLASSIFICATION OF ABSTRACT	20. LIMITATION OF ABSTRACT
UNCLASSIFIED	UNCLASSSIFED	UNCLASSIFIED	UL

DTIC QUALITY INSPECTED 3

Final Technical Report

May 1, 1994 - August 31, 1997

Absorption, Backscatter and Mirror Reflection from Laser and Microwave Plasmas

J.E. Scharer, Principal Investigator
Department of Electrical and Computer Engineering
University of Wisconsin
Madison, WI 53706

September, 1997

DTIC QUALITY INSPECTED 8

Final Technical Report
Absorption, Backscatter and Mirror Reflection
from Laser and Microwave Plasmas
University of Wisconsin
For AFOSR Grant No. F49620-94-1-0054
September, 1997

Abstract

Research on an improved 8-10 GHz microwave system for propagation, reflection and absorption studies of VUV excimer laser (193 nm) produced plasmas has been carried out. Research on the creation of a laser produced sheet plasma for use as either an absorptive layer or a low loss, rapidly scanable agile microwave surface is described. We have installed a new higher energy (300 mJ/20 ns pulse), higher rep rate (20 Hz) laser for our current studies. We have obtained high density $n_e = 2 - 5 \times 10^{13}/cm^3$ laser-formed plasmas which are 9 cm wide $\times$ 40 cm long $\times$ 3-20 mm thick and demonstrated that diffusion is small for time scales less than a microsecond. We have measured the phase and amplitude of microwave reflections and compared it to the same area size aluminum sheet. Preliminary results show that the initial high density plasma ($\hat{n} = 2 - 5 \times 10^{13}/cm^3$) obtained in TMAE at 30–60 mTorr pressures has a reflection coefficient comparable to aluminum and that the recombination coefficient agrees with earlier results of Stalder and Eckstrom. We have also developed a new analysis for the inclusion of Langmuir probe sheath motion in the interpretation of the fast ($\tau \gtrsim 7$ ns) diagnostic. It yields plasma densities in the range of $2 \times 10^{12}/cm^3 - 1 \times 10^{11}/cm^3$ and plasma electron temperatures of 0.8-0.5 eV from 100 ns - 1000 ns after the laser pulse initiation. We have also carried out computer simulations of profile effects on radiofrequency antenna coupling and heating for argon and air plasma utilizing the helicon mode. We have constructed a radiofrequency plasma source facility for studies of sustainment of laser initiated plasmas. We also discuss our collaborations with other research groups and our theoretical and computational research to support and interpret the experimental observations.

I. Introduction.

The experimental and theoretical research carried out over the past year involves creation of plasmas to provide an agile mirror for airborne or shipboard scanning of microwave and millimeter wave systems and creation of collisional absorbing plasmas to reduce 1-10 GHz radar transmission and reflection from objects located in the earth's atmosphere. This type of scheme could also be used to obtain large aperture antenna configurations. By changing the gas mixture to increase collisionality it could also be used as a microwave absorber to reduce radar cross sections. The research topics addressed include VUV (vacuum ultraviolet λ = 193 nm) excimer laser creation of agile mirror reflecting plasma layers and associated theoretical and computational modelling and data analysis for mirror reflection and backscatter as well as plasma sources to elucidate experimental observations and to predict future experimental results.

We have carried out experimental measurements on a sheet beam excimer laser created plasma to study microwave reflection and absorption. Custom designed and fabricated VUV compatible cylindrical lenses are used to produce a 3-20 mm $\times$ 110 mm laser beam (λ = 193 nm, w = 5-300 mJ, τ = 17 ns) for ionization of an organic gas ($n_e \geq 2 \times 10^{13}/cm^3$) to produce a microwave agile plasma surface.

We have published a paper [1] on the plasma properties (n, T) produced by the laser and measured the laser attenuation, photon absorption cross section, plasma diffusion and recombination rates. We have developed a fast Langmuir probe diagnostic ($\tau \gtrsim 7$ ns) and developed a theory to interpret ion saturation currents which include sheath motion to determine the correct plasma density. We have submitted a paper on this to the Journal of Applied Physics [2]. We have also shown that the microwave (10 GHz) reflection properties of the plasma at high density are comparable to those of an aluminum sheet. We have benefited from our interactions and visits with Drs. Stadler, Eckstrom and Vidmar of the Stanford Research Institute on the low ionization energies of organic gases and their use for microwave absorption. We are continuing to discuss our research with Drs. Meger and Mannheimer of NRL, and Dr. Adams of Sandia who are interested in the topic of laser-formed plasmas.

We have published [3] an article involving theoretical and computational research on radiofrequency plasma sources and the effects of antenna coupling, plasma profiles and a fast electron component on wave absorption. This research has provided a computer model basis for the design of our radiofrequency plasma facility. We have also collaborated with Drs. Smithe and Goplen of the Mission Research Corporation in Alexandria, Virginia regarding the use of the MAGIC code for modelling and analysis of two and three dimensional descriptions of microwave radiation from a helix and test antenna backscatter in a plasma column.

Our research group consists of Professor J. Scharer, Dr. M. Bettenhausen and graduate students Kurt Kelly and Guowen Ding who are currently working on this research towards a Ph.D. degree.

II.   Fast Langmuir Probe Measurements in a Laser Produced Plasma

A plasma of high density (> 10^{13} cm^{-3}) and large size (1.3 cm × 9 cm × 45 cm) has been created by a single 20 ns pulse vacuum-ultra-violet laser ionization of the organic gas tetrakis (dimethyl-amino) ethylene (TMAE). Figure 1 illustrates the overall experiment. The dominant plasma decay process is found to be the ion-electron two-body recombination process [4]. The important influence of sheath motion of the decaying plasma for interpretation of Langmuir probe (LP) measurements is also found, which is absent in a steady-state plasma.

In this report, the decaying plasma effect on the interpretation of LP measurements are focused on the 100 ns ~ 1000 ns time scale, because the physical processes at this stage are much simpler than those for t < 100 ns, when the transient ion current, displacement current as well as laser effects on the probe are expected to be important. For our experiment, the decaying plasma is created by a 193 nm wavelength excimer laser ionization of TMAE, with 75 mTorr TMAE pressure and 3 mJ/cm^2 laser pulses.

The decaying plasma effect on the LP measurements primarily comes from the probe sheath motion as the plasma decays, which produces an additional current. Incorporating this effect, a new formula is derived [2] to calculate the plasma density from the probe current density. The relationship between the Bohm current density J_B and the probe current density J becomes

$$J_B = \frac{J}{1 + \dfrac{1}{\sqrt{T_e}}\sqrt{\dfrac{4}{9}\sqrt{2eM_i\varepsilon_0}\ V^{3/2}\dfrac{d(1/\sqrt{J})}{dt}}}$$

(1)

where T_e is the electron temperature, M_i is the ion mass, and V is the sheath voltage. Thus the plasma density can be obtained from the Bohm current density J_B as in a normal LP in a steady-state plasma.

Equation (1) is useful under the condition that the plasma density decay is neither too slow nor too rapid. If the plasma decay is very slow, this means that

$$\frac{1}{\sqrt{T_e}}\sqrt{\frac{4}{9}\sqrt{2e\ M_i\varepsilon_0}\ V^{3/2}\ \frac{d(1/\sqrt{J})}{dt}} \quad << 1$$

then Eq. (1) reduces to $J_B = J$, which is the result for a normal Langmuir probe in the steady-state. The sheath motion effect is very small and no corrections are needed. On the other hand, if the plasma decay is too rapid such that the change in the plasma density Δn on the time scale of the inverse ion plasma frequency is comparable with the plasma density, n, then the Child-Langmuir law is invalid, and so is Eq. (1).

300 mJ 193 nm Excimer Laser used as ionizing source

Lens system is enclosed in a box filled with Nitrogen gas to enhance laser intensity

Microwave alignment is performed with a precison alignment system

Mechanical Rotary Vane Pump is used to evacuate chamber to ~10 mTorr

Backing/Roughing Valve is used To control mechanical pump

TMAE is introduced to the system by means of a needle valve. TMAE vapor pressure is 150 mTorr at room temperature

Langmuir Probe diagnostic system

A Thermocouple gauge and cathode tube are used to monitor pressures

A diffusion pump is used in combination with the mechanical pump to evacuate chamber to ~10E-6Torr

Fig. 1 Laser Plasma Facility

4

The probe current density J can be obtained from the measured probe current, I_m, by correcting for the collecting area, which is larger than the probe area due to probe edge effects for our small planar double-sided disk probe [2]

$$\frac{I_m}{2\pi\, r^2} = J\left(1 + \frac{\pi}{r}\sqrt{\frac{4}{9}\varepsilon_0}\sqrt{\frac{2e}{M_i}}\frac{V^{3/4}}{\sqrt{J}}\right)$$

(2)

where r is the radius of the probe disk.

The experimental probe current (dark curve) and the corrected current (gray curve) are shown in Fig. 2(a), and their ratio is shown in Fig. 2(b). The current corrections arise from both sheath motion effects and probe edge effects, and are equal to the calculated Bohm current density times the probe area. The current ratio is relatively uniform versus time in Fig. 2(b), but the corrections for either sheath motion or the probe edge effects are not uniform.

The sheath motion effects are more important at earlier times than at later times, since sheath motion is more rapid at earlier times. On the other hand, probe edge effects are smaller at earlier times than at later times, since the sheath width is smaller for the higher plasma densities at early times. The two effects cause the current ratio to be relatively uniform in time.

The probe I-V characteristics, before and after the corrections are shown in Fig. 3. It is easy to see that the corrected ion currents are much lower depending on the bias voltage. This agrees with the notion that ion saturation current is independent of bias voltages.

Utilizing this technique, we have measured TMAE plasma densities and have calculated its recombination coefficient $\alpha = 8.6 \pm 1.5 \times 10^{-6}$ cm^3/s for T_e in the range of 0.4 ~ 0.6 eV during the t = 100 - 1000 ns period. This agrees with the result of $\alpha = 9.0 \pm 1.1 \times 10^{-6}$ cm^3/s for room temperature TMAE measured utilizing a microwave method by Stalder and Eckstrom [5].

III.   Microwave Interactions with the Laser Formed Plasma

This section presents a theoretical model of propagation of plane waves through a plasma which we are using to aid interpretation of our microwave scattering experiments. The dispersion relation for plane wave propagation in a plasma is

$$k_p^2 c^2 = \omega^2 - \frac{\omega\, \omega_{pe}^2}{\omega + j\nu}$$

(1)

in which ω_{pe} is defined as the electron plasma frequency

$$\omega_{pe}^2 = \frac{e^2 n_e}{m_e \varepsilon_0}$$

(2)

5
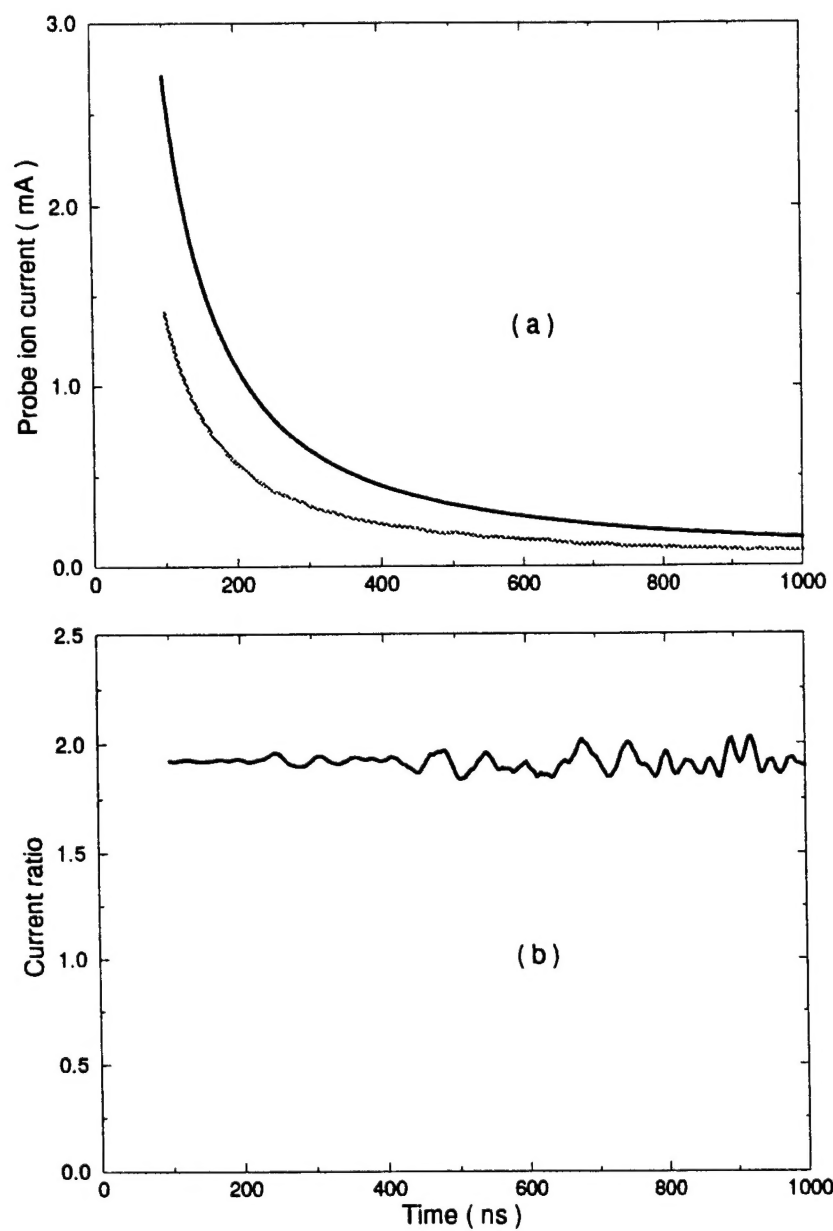
Figure 2.(a) Probe ion saturation current and its correction for both sheath motion and probe edge effects. (b) Ratio of the probe current and its correction (the bias voltage is -45 V.)
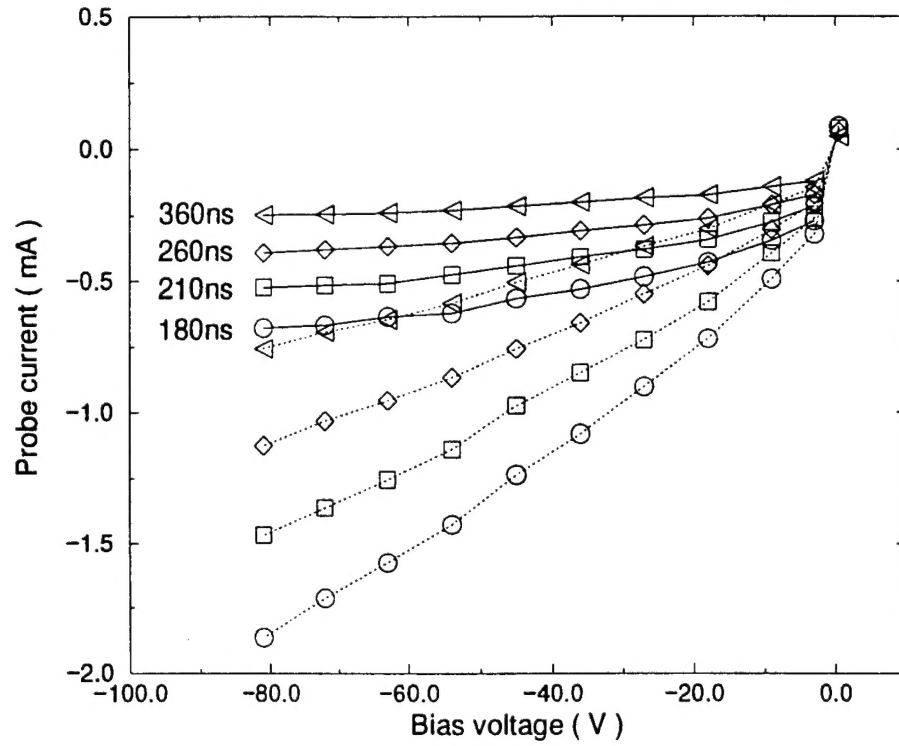
6

Figure 3. Probe I-V characteristics, before (dotted line) and after corrections (solid line) for both sheath motion and probe edge effects. (Various delay time from the initial laser pulse at 360 ns, 260 ns, 210 ns and 180 ns, respectively)

and ν is the electron-neutral collision frequency. The complex propagation constant k is defined as

$$k_p = \beta_p + j\alpha_p \qquad (3)$$

The wave attenuates according to α_p and propagates according to β_p.

Dielectric Slab Model

      Propagation of plane electromagnetic waves through a dielectric slab of thickness d is illustrated in Fig. 4. By matching boundary conditions at 0 and d and solving for the ratios of incident, reflected and transmitted power, power refection and transmission coefficients are obtained. If there is free space above and below the plasma, the dielectric model predicts a reflection coefficient from the left interface of the plasma of

$$R = |R|e^{j\phi} = \frac{\eta_p - 1}{\eta_p + 1} \qquad (4)$$

where η_p is the impedance transformation of free space through the plasma

$$\eta_p = Z_p \times \frac{1 + Z_p \tan h(k_p d)}{Z_p + \tan h(k_p d)} \qquad (5)$$

and

$$Z_p = \frac{1}{1 - \dfrac{\omega_p^2}{\omega(\omega + j\,\nu)}} \qquad (6)$$

is the impedance of the plasma. R and ϕ are the magnitude and phase, respectively, of the reflection coefficient for the free space - plasma interface. By measuring R and ϕ for many values of d it is possible to solve for k_p. From this we can solve for n_e and ν using Eq. (2).

The Budden Model

      Although the dielectric slab description is accurate for a homogeneous plasma, it was determined that there were several areas that this model was inaccurate. The plasma is thought to diffuse a small amount making for a non uniform plasma density profile. In experiments by Shen, Scharer, Porter, Lam and Kelly [1], the plasma was determined to not have a step profile as in the dielectric slab, but rather a peak density near it's center, with a somewhat less dense plasma near it's edge. Budden has solved the wave equation for a dielectric with just such a profile. This theory gave a closed form solution for the reflected and transmitted waves and could account for different densities as well as a wide range of collision
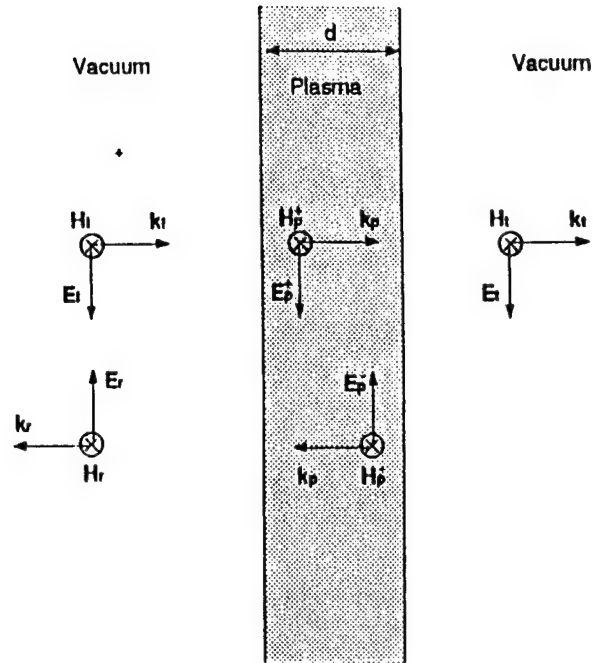
8

Figure 4. Plane waves incident on a dielectric slab of thickness d

frequencies. Either low loss reflection or highly lossy absorbers can be treated with this formalism.

The Budden Model is based on a solution to the hypergeometric equation:

$$\zeta (1-\zeta) \left(\frac{d^2 u}{d^2 \zeta}\right) + \left\{ c - (a+b+1)\,\zeta \right\} \frac{d u}{d \zeta} - abu = 0 \tag{7}$$

If we let

$$- \zeta = e^Z \tag{8}$$

and

$$Z = (z / \sigma) \tag{9}$$

the hypergeometric equation is transformed into:

$$(1 + e^Z) \frac{d^2 u}{d^2 Z} + \left\{ c - 1 + (a+b)\,e^Z \right\} \frac{d u}{d Z} + abe^Z\, u = 0 \tag{10}$$

This is transformed into its normal form by substituting

$$u = E\, exp \left\{ \frac{1}{2}(1-c)(Z) \right\} (1 + e^Z)^{(c-1-a-b)\ /2} \tag{11}$$

where E will be used to denote the electric field. We now obtain the wave equation:

$$\frac{d^2 E}{d^2 z} + k^2 q^2 E = 0 \tag{12}$$

where

$$q^2 = \varepsilon_1 + \frac{e^z}{(e^z + 1)^2} \left\{ (\varepsilon_2 - \varepsilon_1)(e^z + 1) + \varepsilon_3 \right\} \tag{13}$$

and

$$\varepsilon_1 = -\frac{1}{4} \frac{(c-1)^2}{\sigma^2 k^2} \tag{14}$$

$$\varepsilon_2 = -\frac{1}{4} \frac{(a-b)^2}{\sigma^2 k^2} \tag{15}$$

$$\varepsilon_3 = \frac{1}{4} \frac{(a+b+1-c)(a+b-1-c)}{\sigma^2 k^2} \tag{16}$$

10

If we substitute the following parameters for a, b, and c:

$$c - 1 = -2ik\sigma \cos^2(\theta) \tag{17}$$

$$a - b = -2ik\sigma q_0 \tag{18}$$

$$a + b - c = \pm(4k^2\sigma^2\varepsilon_3 + 1)^{1/2} \tag{19}$$

we get a closed form solution of the wave equation for the reflected and transmitted waves.

It can be seen that if we let

$$\varepsilon_1 = \varepsilon_2 = \cos^2\theta \tag{20}$$

and

$$\varepsilon_3 = \frac{-4X_m}{1 - iZ} \tag{21}$$

we get a dielectric constant of a plasma with density profile given by

$$X = X_m \, sech^2\left(\frac{z}{2\sigma}\right) \tag{22}$$

and a collisonality given by

$$Z = \frac{\nu}{\omega} \tag{23}$$

The parameter σ can be thought of as a thickness parameter. The reflection and transmission coefficients become

$$R = \frac{(-2ik\sigma \cos\theta)! \, (2ik\sigma \cos\theta - \gamma - \frac{1}{2})! \, (2ik\sigma \cos\theta + \gamma - \frac{1}{2})!}{(2ik\sigma \cos\theta)! \, (-\gamma - \frac{1}{2})! \, (\gamma - \frac{1}{2})!} \tag{24}$$

and

$$T = [[2ik\sigma \cos(\theta)] \frac{\left[2ik\sigma \cos(\theta) - \gamma - \frac{1}{2}\right]! \left[2ik\sigma \cos(\theta) + \gamma - \frac{1}{2}\right]!}{[[2ik\sigma \cos(\theta)!]^2} \tag{25}$$

where

$$4\gamma^2 = 1 + 4k^2\sigma^2\varepsilon_3. \tag{26}$$

11

A computer code was developed to calculate results for Epstein profiles (such as those shown in the bottom plot of Figure 8) and to optimize the experimental conditions. A study of Fig. 5 determined that at a 9 GHz operating frequency, it was desirable to have a sharp boundary to produce a highly reflective plasma. This is consistent with the slab model. An examination of Fig. 6, meanwhile, suggested a more diffuse boundary could produce a highly absorptive plasma. Another important parameter is the collision frequency. Operating at higher neutral pressures could enhance the absorptive properties of the plasma as this would provide a larger neutral density. Also, backfilling the chamber with an inert gas such as argon could lessen the effects of collisionality by decreasing the number of negative ions in the plasma.

Purpose

Radar scanning can be carried out in a number of ways. The simplest example is a single element transmitter scanned mechanically in elevation and azimuth. Such a radar system might work in a few applications in which objects are moving very slowly, or are very far away (astronomical distances). But for most applications, such as for tracking aircraft or missiles, a mechanical scanner is far too slow.
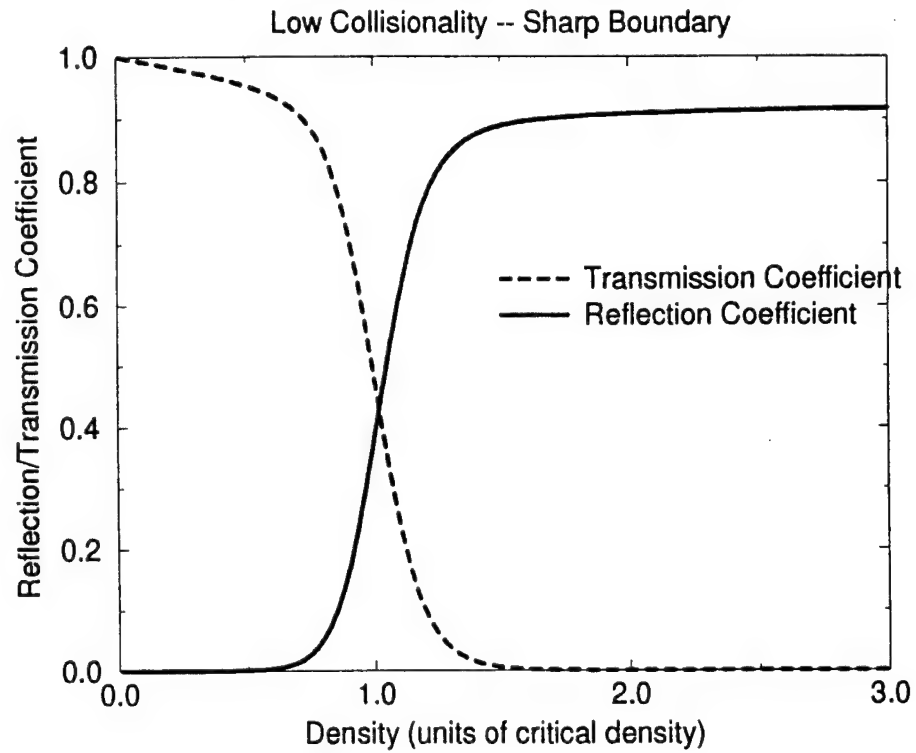
Another way of radar scanning is the use of a phased array. In this case, an array of individual radiating elements are excited with differing phases controlled such that a narrow beam can be scanned. They have no moving parts. Phased arrays have been used for decades in radar applications. They are fast and effective in determining the location and velocity of objects. However they are very large and require large amounts of power and microwave circuitry to operate. For use on mobile crafts such as a warship, they can be cumbersome.

This report describes some basic research aimed at using a single element horn antenna as a source, reflecting it off a planar plasma sheet for scanning purposes, and yet avoiding the disadvantages of a mechanical moving device. The idea is to optically rotate a plasma reflector. Various methods may be used to rotate the plasma reflector. Researchers at the Naval Research Laboratory use an array of hollow cathodes to start a planar gas discharge. The planar discharge is rotated by applying voltage to a set of electrodes [6]. Another method of rotating a plasma is to generate it with a short pulse laser beam, wait for the ions and electrons to recombine, electrically rotate the laser beam, and then generate a new plasma with another short pulse at the rotated position. The technology for rotating a laser beam exists commercially in the visible spectrum.

In addition, a highly collisional, diffuse plasma can be used for the absorption of microwaves. This is useful to reduce the radar cross-section of targets, essentially hiding them from radar detection systems.
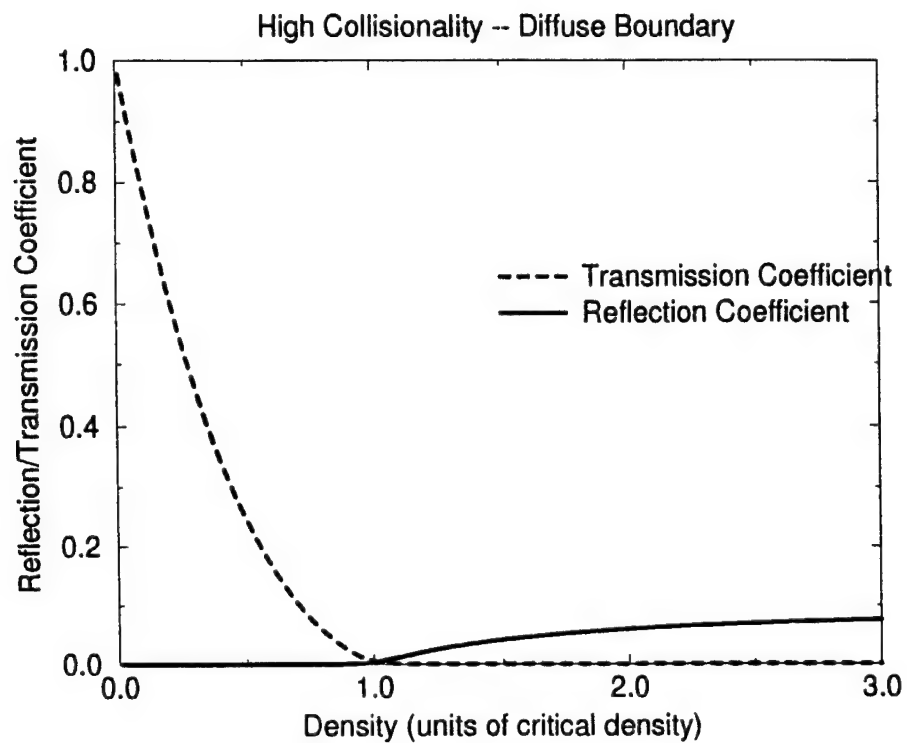
This report considers the feasibility of the laser plasma generation scheme following the work of Shen and Scharer [1] and Zhang and Scharer [7]. It considers properties of the plasma and their effects on its ability to reflect microwave radiation in the X-band.

12

Reflection and Transmission from an Epstein Profile

Low Collisionality -- Sharp Boundary

Figure 5. A sharp boundary $(\sigma = 1cm)$ slightly collisional $(\nu = 90MHz)$ sheet can be highly reflective if it has adequate plasma denstiy.

Reflection and Transmission from an Epstein Profile

High Collisionality -- Diffuse Boundary

Figure 6. A diffuse boundary ($\sigma = 10cm$) highly collisional ($\nu = 1GHz$) sheet can be highly absorptive even at low plasma density.

Description of the Laboratory and Experimental Conditions

The laser radiation is directed into a vacuum chamber containing the organic gas Tetrakis (dimethyl-amino) ethylene (TMAE). The laser ionizes the gas creating a plasma. X-band microwaves are launched from a highly directive horn antenna toward the plasma where they will be partially transmitted and partially reflected. A bi-static antenna system was used for the purposes of isolation.

High Energy Excimer Laser Acquisition and Installation

A new pulsed Ultra-Violet laser was purchased in the summer of 1996. This new laser can produce 300 mJ of VUV laser radiation. This represents a 200 fold improvement in laser power over a laser that was formerly utilized in this lab. The laser has stable output with only 5% shot-to-shot variation. This will make the results of the experiment much more repeatable than in the past. The laser was installed in June 1996. It has a water cooled system to regulate internal vessel pressure and temperature. A new filtration system was needed to provide sufficient water pressure while eliminating corrosive contaminants in the university water system. The vessel contains a mixture of four gases. Hydrogen is used to passivate the system after it has been exposed to atmosphere. The working gas mixture is a combination of Neon, Fluorine, and Argon. The Fluorine is combined with inert Helium in the supply tank for safety purposes. All gas purities are Ultra-High for superior laser performance. A new gas handling system was installed at the same time as the laser to insure sterility.

The laser power supply is contained in the main housing. It was necessary to construct a reinforced table to support the 200 kg unit. Power is supplied by a 3 phase, 110 Volts / phase cable capable of delivering 20 amps. The laser is capable of a 20 Hz repetition rate. Output energy is regulated by an internally calibrated photo-diode. Capacitor voltages and filling pressures are adjusted by internal feedback systems to ensure stable output.

The excimer laser is being operated at 193 nm with the use of Argon Fluoride. Some of this energy is lost in the UV windows and O_2 absorption in air. Our preliminary measurements show that 5% of the radiation is lost to the windows. Further experiments have suggested that the laser energy decreases by 1.5 db / meter due to oxygen absorption. We have a vacuum chamber for the lenses which can be filled with an inert gas to reduce these losses and therefore utilize more of the available laser energy.

Lenses and Vacuum Chamber

Most of the laser beam is contained in a region 15 × 30 mm at the laser output window. With a series of four custom designed and fabricated Suprasil lenses manufactured by Midwest Optics, the laser beam can be adjusted to be (3-7)mm × 3-11) cm. Figure 7 is a diagram illustrating the lenses set to generate a 2 mm × 11 cm beam. The lenses are located in an aluminum box near the laser output window. It is hoped that the new channel will extend the lifetime of these lenses. It was determined that a typical lens has a 2-6 year lifetime due to degradation of the VUV coating. With the new higher power laser, this degradation has been observed. An

15

Output Laser beam
1.4 mm thickness

Input
193 nm
laser beam

22 mm x 7 mm
cross section

Width = 11.0 cm
Height = 3.5 cm
F = 18.4 cm

Width = 3.5 cm
Heigth = 3.5 cm
F = -3.69 cm

Width = 3.5 cm
Heigth = 3.5 cm
F = - 3.69 cm

Width = 3.5 cm
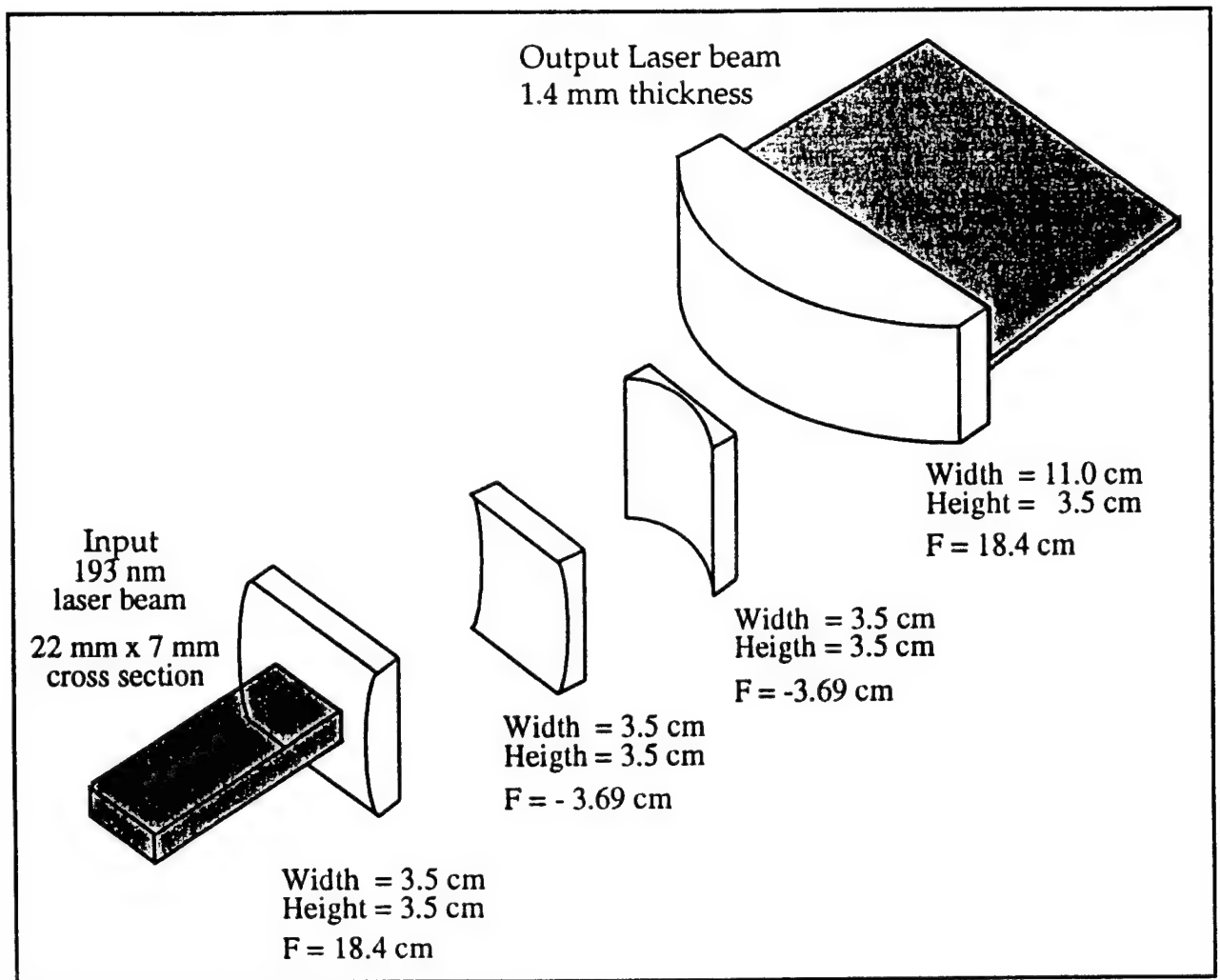Height = 3.5 cm
F = 18.4 cm

Figure 7. Lens system to form sheet profile

aperture located between the third and fourth lenses - referenced from the laser side - can make the beam sharp in the y-direction. This is desirable because stray light outside the main laser beam can cause the plasma to be underdense in the region above and below the main plasma sheet. A sharp plasma boundary is desirable so as to approximate a piece of sheet metal. Approximating a sheet of metal is desirable since metal will be used as a 100% amplitude and 180° phase reflection reference.

The vacuum chamber is a 6 inch Corning glass T which is evacuated to 10^{-6} Torr. This ensures TMAE vapor purity. The vapor pressure of TMAE is 350 mTorr at room temperature. Typical filling pressures are 60 - 100 mTorr. A new chamber was constructed by University of Wisconsin Physical Science Labs in Fall 1996 which will allow for microwave windows. The new chamber is constructed of stainless steel. Several layers of absorptive paint will be applied to reduce extraneous reflections. The chamber was designed such that it can be supported and utilized with minimum reflections from vacuum pumps and instrumentation which would normally interfere with accurate measurements.

Plasma Conditions

The first ionization potential of TMAE is 5.36 eV. A photon of wavelength 193 nm has an energy of 6.40 eV. Consequently, for single photon ionization, an electron temperature of about 1 eV can be expected initially. It is expected that collisions will reduce this value after a laser pulse has ended. Langmuir triple probe measurements [9] indicate that this is the case.

The plasma profile in the y-direction was measured with a planar circular disk Langmuir probe. A typical profile is shown in the top plot of Figure 8. This profile was done with the aperture adjusted to 6 mm and the lenses adjusted as shown in Fig. 7. For these measurements, a reference probe was placed near the laser beam and left in a constant position while a mobile probe was scanned in the y-direction.

Microwave Homodyne Detection System

This section presents the microwave waveguide circuit used to measure the reflection off of and the transmission through the plasma. It also includes the basic theory for microwave detection and how it is applies to the circuit.

Components

Figure 9 shows the waveguide system designed to measure the amplitude and phase of the transmitted signal and reflected signals. All experiments were done with X-band microwaves using an HP Model 620A SHF Signal Generator. This is a tunable source with a peak output of about 100 mW of power. For frequency measurements more accurate than the generator dial could indicate, an HP model 532B Frequency Meter was used. It was inserted directly after the first coax to waveguide transition from the generator. Accurate frequency measurements were important primarily to assure that the frequency was not drifting during an experiment. Reflections from microwave components as well as from objects in the lab would change with changes in frequency. It was therefore useful to be able to

Hyperbolic Secant Squared Profile

Thickness of profile is governed by parameter σ.
A diffuse boundary corresponds to a large value of σ.
A somewhat sharper boundary is characterized by a
smaller value of σ. An actual density profile is shown
for comparison.
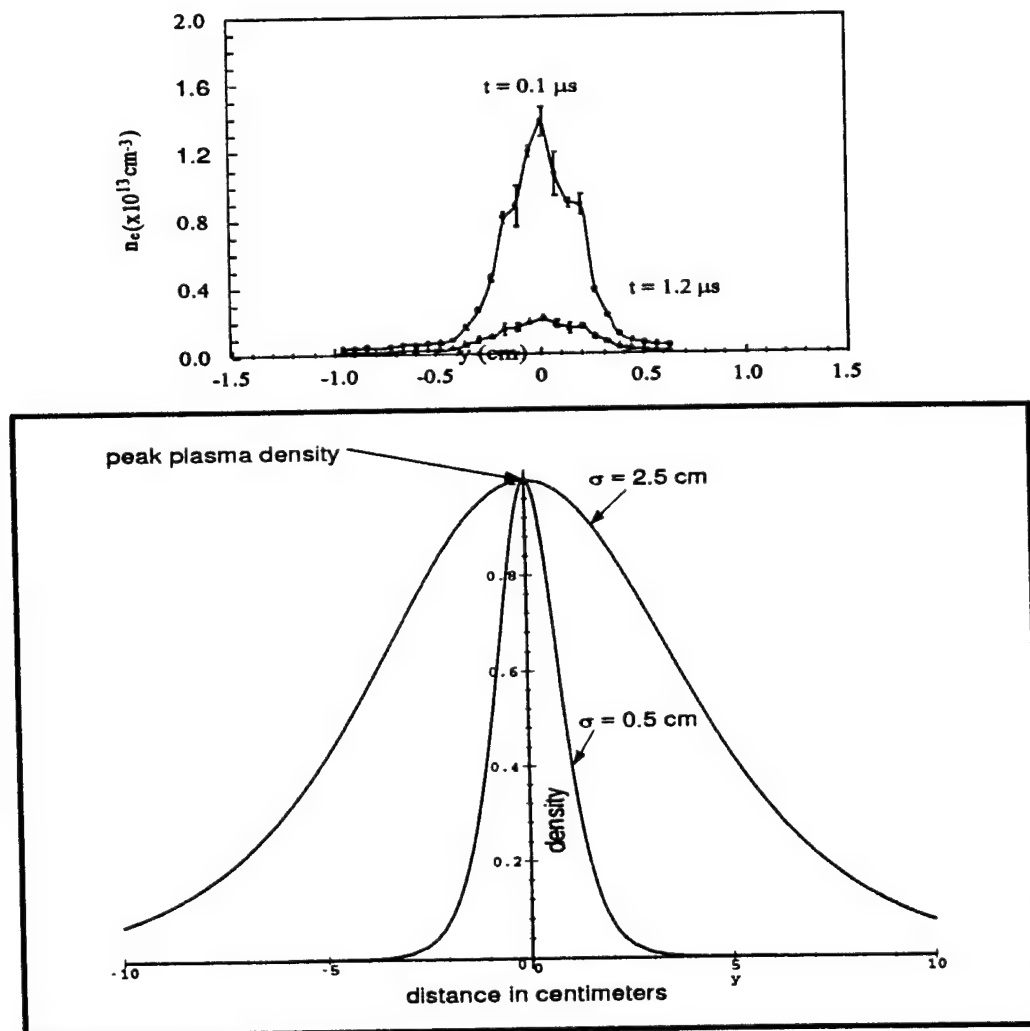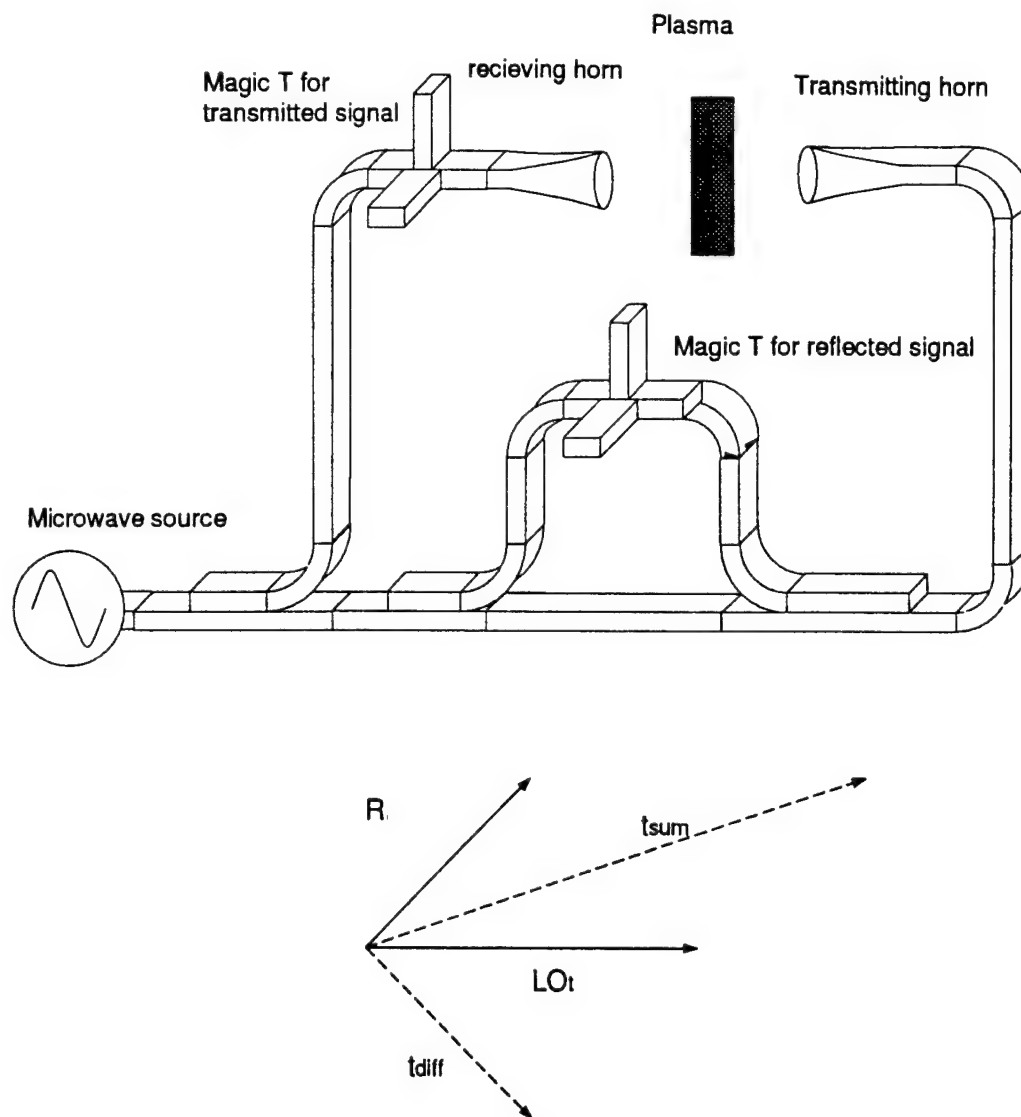

Figure 8. Plasma Density y-profile and Corresponding Epstein Profile

Figure 9. X-band reflectometer/interferometer to measure reflection/ transmission from/through a plasma along with phasor signal representation.

check the exact frequency during calibration and then after the experiment to make sure it did not drift.

Obtaining amplitude and phase from the circuit

It is useful to consider the signals in phasor notation. Figure 9 demonstrates this. Before the laser shot, LO and R are in phase. After, the laser fires and a plasma is produced, there is a change in both the amplitude and phase of R. To obtain the phase of the reflected signal, ϕ, $|R|$ is first solved for:

$$|R| = \sqrt{t_{sum}^2/2 + t_{diff}^2/2 - LO_t^2} \quad . \tag{27}$$

The phase of the reflected signal is then found with the law of cosines

$$\phi = \pi - \cos^{-1}\left(\frac{t_{sum}^2 - |R|^2 - LO^2}{-2|R|LO}\right) . \tag{28}$$

Microwave Heterodyne Detection System

Another method of obtaining amplitude and phase information is by using a heterodyne detection system. The heterodyne system we used utilized two microwave sources separated in frequency by 50 MHz. The second source was a HP 8690B Sweepable generator which was purchased in December 1995. As with the homodyne system, a Magic T functions as an interferometer. Each of two Magic T's will mix two signals. One of these signals will be the upper frequency common to both T's. On one of the T's the other signal will be a reference which does not pass through the plasma. The output on this diode is just a 50 MHz signal with a phase that can be adjusted with a phase shifter. The other T will detect the signal which has traveled through the plasma. The output on its diode will be a 50 MHz signal with a time varying amplitude and a time dependent phase. For the purposes of analysis, it is necessary to assume that the phase shift is a constant over one period of the intermediate frequency (IF). This assumption places a limit on the time response of the system. The two signals are compared. This method is superior because Fourier transform techniques can be used to filter all but the 50 MHz signal. In addition, the phase of the reflected signal is a directly measurable quantity. The shortcoming of this procedure is a much slower time response if phase is to be known with a high degree of accuracy. This is caused by limitations of the oscilloscope sampling rate.

For example, let the sampling rate of the scope be denoted by SF. The number of data points upon which one can accurately measure the phase is just:

$$n = \frac{SF}{IF} \tag{29}$$

However, the error by which the phase is known is given by

$$\Delta\phi = 2\pi\frac{IF}{SF} = 2\pi\frac{1}{n} \tag{30}$$

From this expression it is easy to see that the more accurate determination of ϕ corresponds to a larger IF. But a larger number of data points corresponds to a smaller IF This was a determining factor in choosing 50 MHz for our intermediate frequency. It allowed us to get time resolution of 20 nanoseconds and a determination of the phase to within 6°.

Obtaining amplitude and phase from the circuit

The analysis of data is much less cumbersome with the heterodyne system. The amplitude of the reflected signal is simply the Fourier amplitude of the 50 MHz signal on the diode. The phase of the reflected signal can be found using the reference diode. Before the experiment begins, a phase shifter is used to adjust the reference signal to match the phase of a signal being reflected off an aluminum sheet. This will be assumed to be 180°. During a typical laser shot there will be a time delay Δt between the reference signal and the signal being reflected from the plasma interface. The phase of the reflected signal is given by:

$$\phi = \pi - IF\,\Delta t \tag{31}$$

Figure 10 shows reflection data for plasmas created at 2 different neutral TMAE pressures. Data was collected using a homodyne detection system and normalized to reflection levels obtained by placing an aluminum sheet in the same position as the plasma. The higher pressure plasma (P = 60 mTorr) reaches its maximum reflectivity at a time of t = 250 ns. While the lower pressure (P = 40 mTorr) reaches its maximum at t = 350 ns. The laser pulse occurs at t = 100 ns in both cases and has a pulse length of 20 ns. The initial conditions of the plasma sheet show an electron density gradient along the laser axis. This gradient effects the phase of the reflected signal from each differential segment of the sheet. As the gradients vanish in time due to plasma recombination, the sheet becomes more uniform and phase interference from neighboring differential segments decreases. It is at this time that the microwave beam pattern from the sheet is expected to most closely resemble the beam pattern from the antenna.

IV.   Radiofrequency Plasma Source for Sustainment of Laser Produced Plasmas

We have designed and are completing construction of a radiofrequency plasma source experiment to complement our laser plasma research. The initial conclusions of this effort were presented at the ICOPS '97 conference in San Diego, CA. The goal of this work is to investigate radiofrequency excitation as a means of increasing the lifetime of the laser-produced plasma. Our current research plan is:
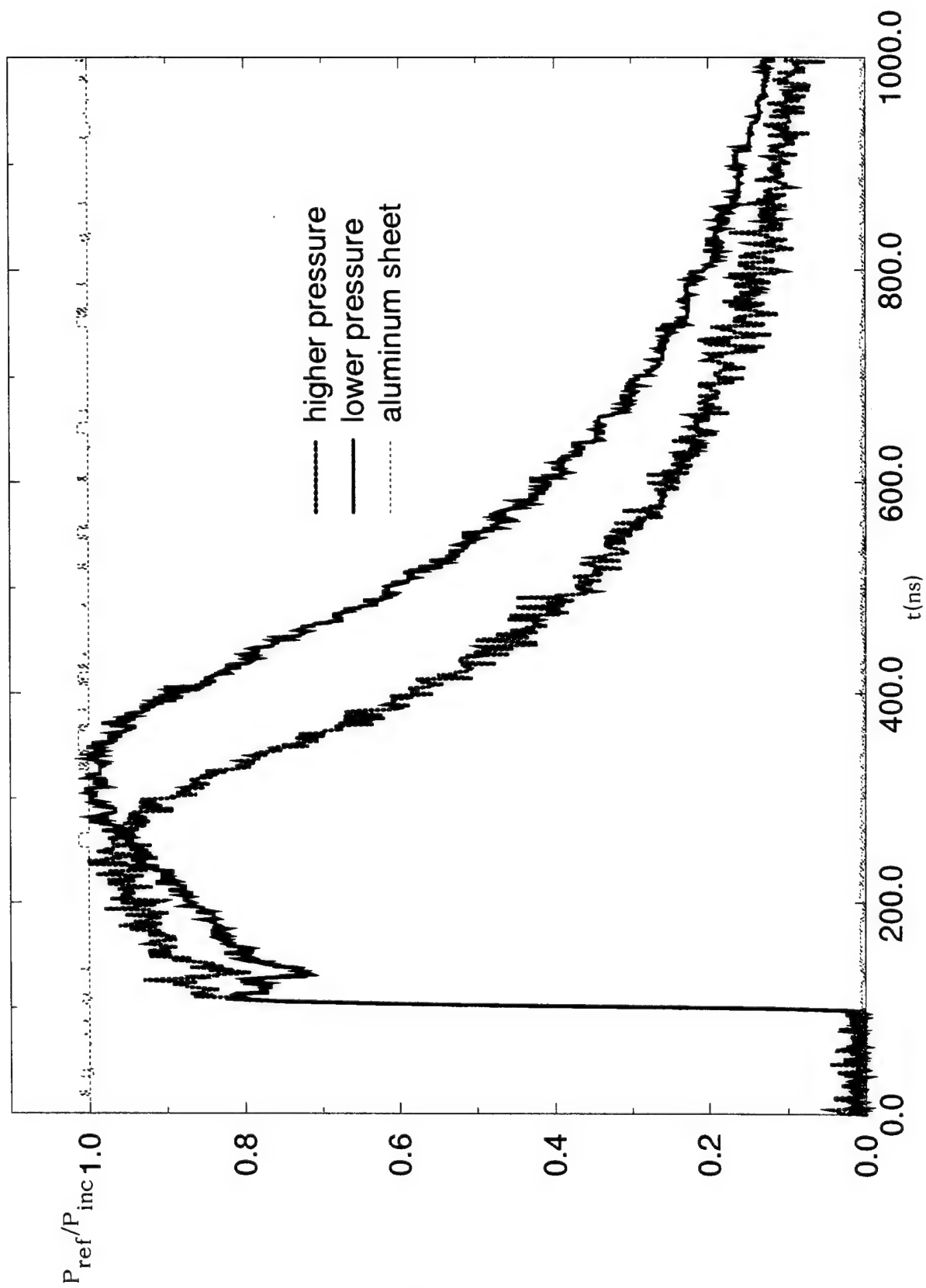
Figure 10. Microwave reflection from laser formed plasma

higher pressure
lower pressure
aluminum sheet

P_{ref}/P_{inc}

1.0

0.8

0.6

0.4

0.2

0.0

0.0   200.0   400.0   600.0   800.0   1000.0

t(ns)

22

1. Investigate RF source operation at 1--100 MHz with inert gases at 1--100 mTorr pressures.
2. Investigate low power RF source operation using low ionization seed gases in a buffer gas.
3. Study RF effects on the lifetime of spark-gap initiated plasmas.
4. Combine the RF source with our laser plasma experiment with low ionization seed gases to investigate RF effects on plasma lifetime and profiles.
5. Investigate recombination and plasma chemistry processes with seed and buffer gas mixes to determine methods to reduce power requirements for maintaining the plasma. This will be extended over time to include issues relating to atmospheric air plasma sustainment.

Figure 11 shows a schematic of the RF/laser plasma system design. Our laser provides up to a 300 mJ pulse at 193 nm. Scaling from our earlier results with a 10 mJ laser suggest that we will be able to produce a 40 cm long, 10 cm diameter cylindrical plasma with above critical densities with our current laser. We will use a new optical system to expand the laser beam to the size and shape needed to create the cylindrical plasma. We plan to use an RF generator operating in the range 1--100 MHz. Various operating frequencies in that range will be used to study the frequency dependence with various gas mixtures, plasma collisionality, and magnetic field. Our magnets are capable of providing a solenoidal magnetic field up to 1400 Gauss. We plan to operate primarily in the 0--300 Gauss range.

We have done some antenna coupling modeling using our ANTENA2 and MAXEB codes [3] and the parameters discussed above. Figure 12 shows that at high density ($n = 5 \times 10^{12}/cm^3$) and collisionality ($v = 10^8$ Hz) and low magnetic field ($B = 50$ G), the power absorption for 13 MHz is very near the antenna. For a higher magnetic field ($B = 250$ G) and the same plasma parameters, Fig. 13 illustrates that the radiofrequency wave fields and power absorption propagate well away from the antenna. These studies suggest that radiation resistances should be on the order of 0.4--0.5 Ohms for a Nagoya Type III antenna. This radiation resistance is sufficient for coupling power into the plasma. We plan to conduct further studies to better tailor the antenna design based on measurements of density profiles and collision frequencies from the laser plasma experiment. Later, readily ionized seed gases and an approach towards atmospheric air plasmas will be investigated.
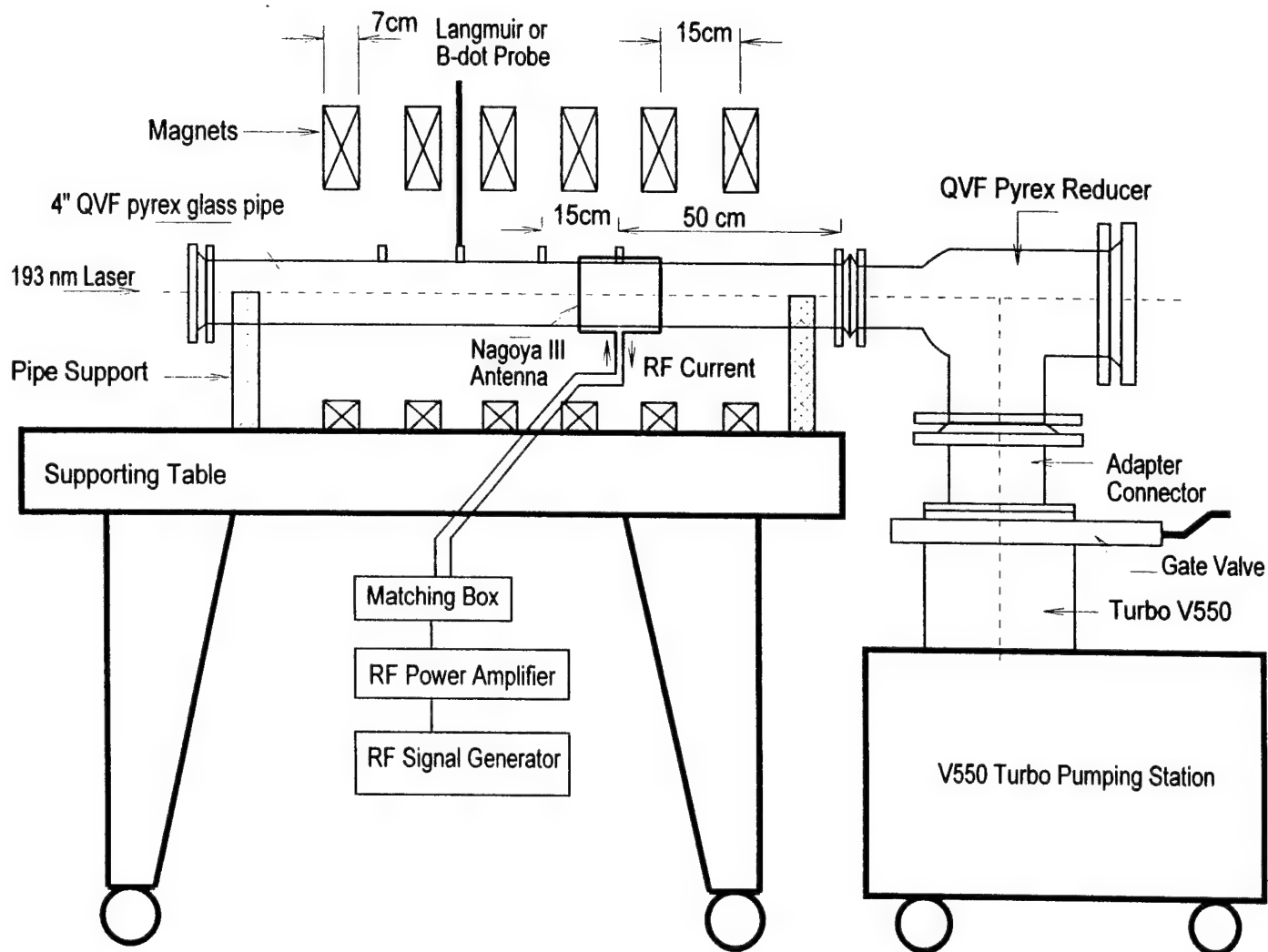
RF Plasma Source
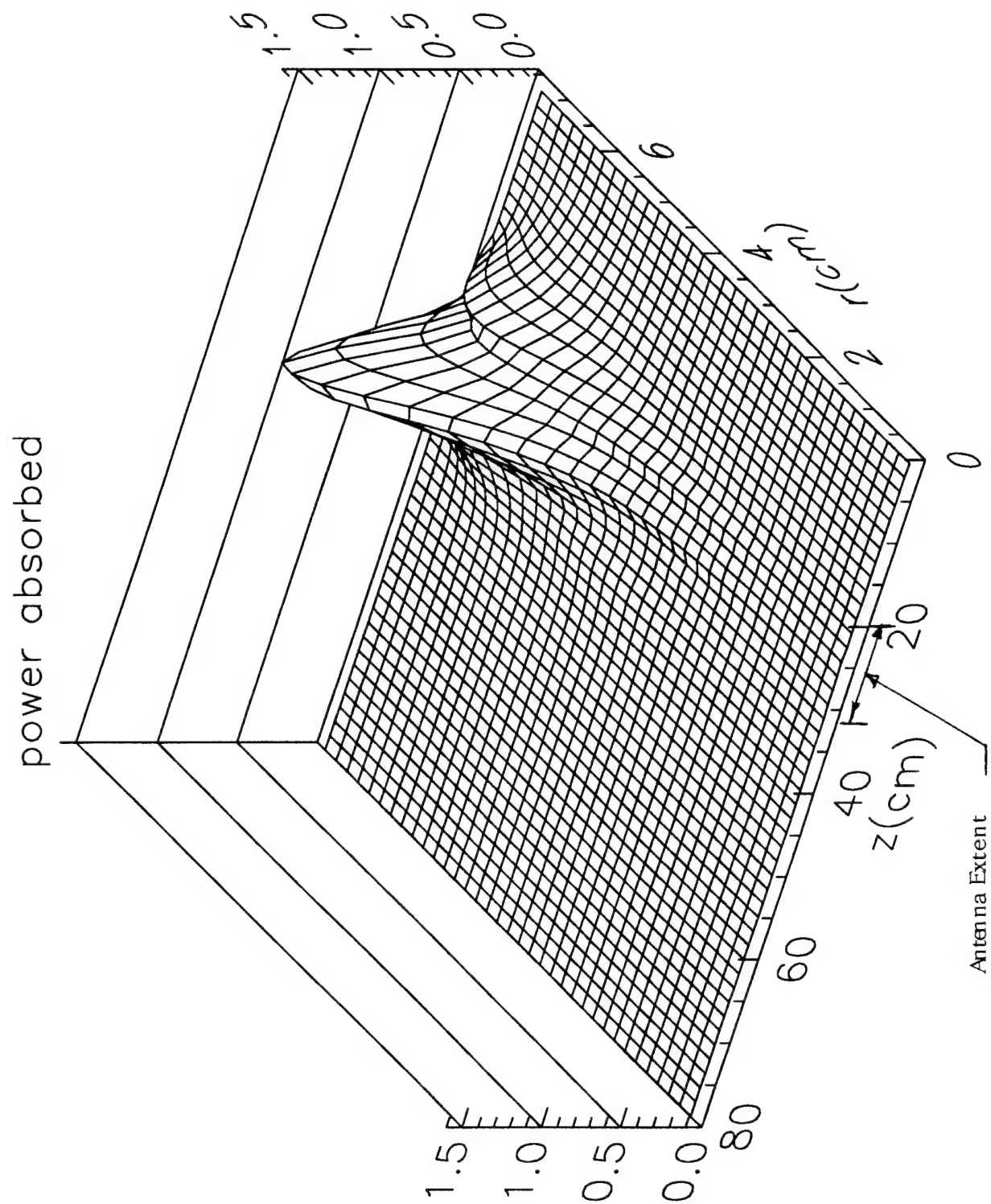

Figure 11.   Radiofrequency Plasma Source Facility

24

power absorbed

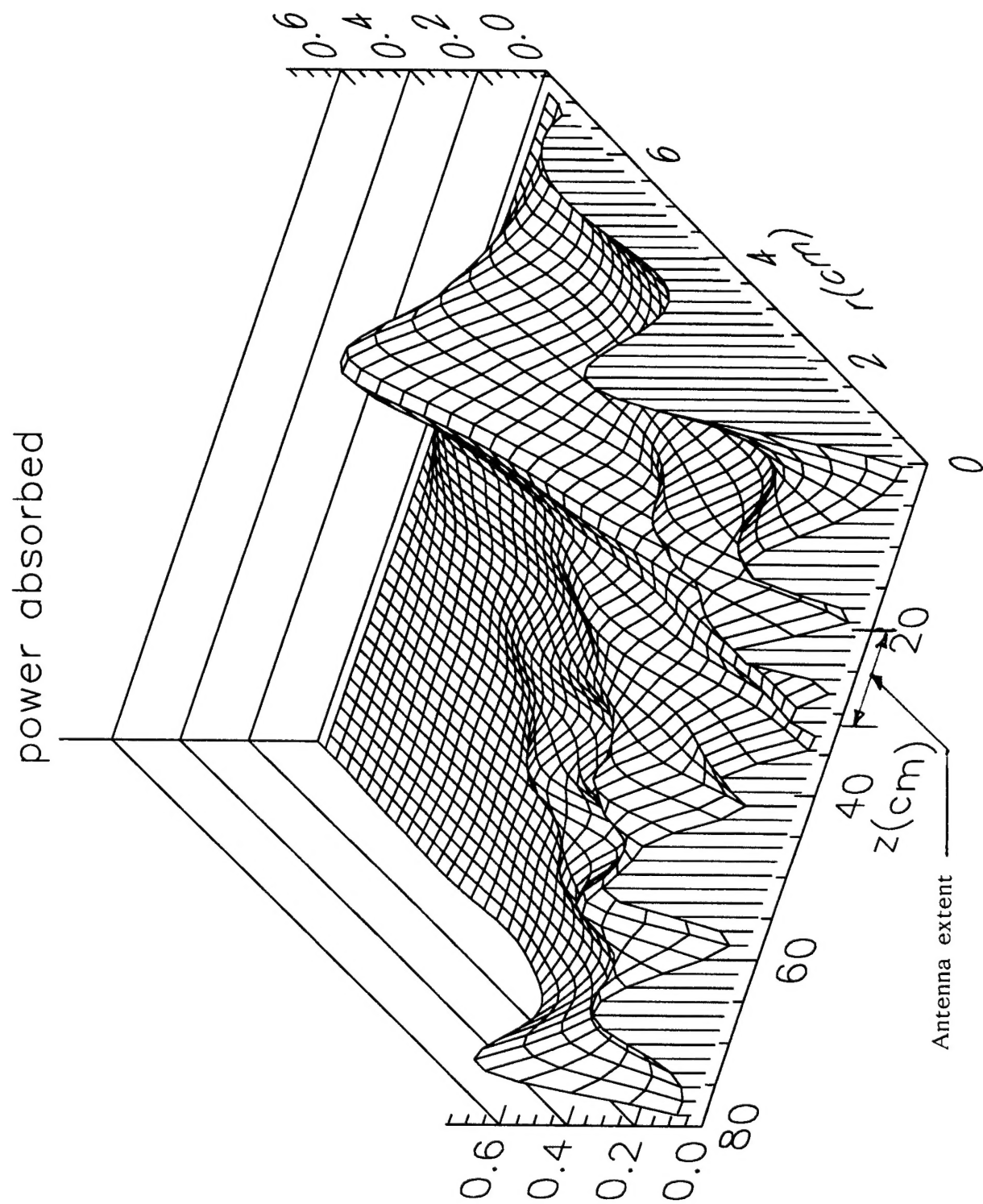Figure 12. Radiofrequency Power Absorption (B = 50 G).

power absorbed

Antenna extent

Figure 12. Radiofrequency Power Absorption (B = 250 G)

References

1. W. Shen, J.E. Scharer, N.T. Lam, B.G. Porter, and K. L. Kelly, "Properties of an Vacuum Ultraviolet Laser Created Plasma Sheet for a Microwave Reflector," Journal of Applied Physics **78**, 6974 (1995).
2. G. Ding, J. Scharer and K. Kelly, "Fast Langmuir Probe Measurements in a Laser Produced Plasma," 22 pages, submitted to Journal of Applied Physics (1997).
3. Y. Mouzouris and J. Scharer, "Modelling of Profile Effects for Inductive Helicon Plasma Sources," IEEE Trans. of Plasma Sciences **24**, 152 (1996).
4. Guowen Ding, M. S. Thesis, University of Wisconsin-Madison, 1997.
5. K. R. Stalder and D. J. Eckstrom, J. Appl. Phys. **72** (9), 3917 (1992).
6. R.A. Meger, J.A. Gregor, R.E. Pechacek, R.F. Fernsler, and W. Manheimer, "Experimental investigations of the formation of a plasma mirror for high frequency microwave bean," Physics of Plasmas - APS-DPP 1994 special issue (1994).
7. Y.S. Zhang and J.E. Scharer, "Plasma generation in an organic molecular gas by an ultraviolet laser pulse," Journal of Applied Physics **73** (10), 4779 (1993).

VII. Publications (1994-97)

A. Journal Articles

1. W. Shen, J.E. Scharer, N.T. Lam, B.G. Porter, and K. L. Kelly, "Properties of an Vacuum Ultraviolet Laser Created Plasma Sheet for a Microwave Reflector," Journal of Applied Physics **78**, 6974 (1995).
2. Y. Mouzouris and J. Scharer, "Modelling of Profile Effects for Inductive Helicon Plasma Sources," IEEE Trans. of Plasma Sciences **24**, 152 (1996).
3. G. Ding, J. Scharer and K. Kelly, "Fast Langmuir Probe Measurements in a Laser Produced Plasma," 22 pages, submitted to Journal of Applied Physics (1997).
4. K. Kelly, J. Scharer, G. Ding and M. Bettenhausen, "Microwave Reflections from a Vacuum Ultra Violet Laser Produced Plasma Sheet," to be submitted to the Journal of Applied Physics (1997).

B. Conference Presentations

1. B.E. Chapman, J.E. Scharer, W. Shen and Y.S. Zhang, "Electron Cyclotron Waves in a Highly Inhomogeneous Plasma," IEEE International Conference on Plasma Science, Santa Fe June 6-8, Record 94CH3465-2 159 (1994).
2. Brian E. Chapman, J.E. Scharer, W. Shen, M.H. Bettenhausen, "Electron Cyclotron Waves in a Highly Inhomogeneous Plasma," Bull. Am. Phys. Soc. **39**, 1550 (1994).
3. B.G. Porter, J.E. Scharer, W. Shen and N.T. Lam, "Microwave Reflection from an XUV Laser Generated Planar Plasma Sheet," Bull. Am. Phys. Soc. **39**, 1551 (1994).
4. Y. Mouzouris, J.E. Scharer, M. Bettenhausen, and W. Shen, "Modelling of Helicon Sources for a Variety of Inductive Coil Antenna Couplers," Bull. Am. Phys. Soc. **39**, 1550 (1994).

5. W. Shen, J.E. Scharer, B. Porter and N.T. Lam, "XUV Laser Produced Plasma Sheet Beam and Microwave Agile Mirror," IEEE International Conference on Plasma Science, Santa Fe June 6-8, Record 94CH3465-2 206 (1994).

6. W. Shen, J.E. Scharer, B.G. Porter, N.T. Lam and Y. Mouzouris, "Experimental Study of XUV Laser Produced Plasma Sheet for a Microwave Agile Mirror Application," Bull. Am. Phys. Soc. 39, 1550 (1994).

7. B.G. Porter, J.E. Scharer, W. Shen and N.T. Lam, "An XUV Laser Generated Planar Plasma Microwave Reflector," IEEE International Conference on Plasma Science, Madison June 5-8, Record 95CH35796, 34 (1995).

8. Y. Mouzouris, J.E. Scharer, and M. Bettenhausen, "Modelling of Profile Effects for Inductive Helicon Plasma Sources," IEEE International Conference on Plasma Science, Madison June 5-8, Record 95CH35796 , 30 (1995).

9. W. Shen, J.E. Scharer, B.G. Porter, N.T. Lam and K.L. Kelly, "Experimental Study of XUV Laser Produced Plasma Sheet for a Microwave Agile Mirror Application," IEEE International Conference on Plasma Science, Madison June 5-8, Record 95CH35796, 34 (1995).

10. Y. Mouzouris, J.E. Scharer, M. Bettenhausen, "Fast Electron Effects on Power Absorption Profile for Inductive Helicon Plasma Sources," Bulletin of the American Physical Society 40, 1679 (1995).

11. Weimin Shen, J.E. Scharer, K.L. Kelly, M.B. Bettenhausen, N.T. Lam, "Experimental Study of VUV Laser Produced Plasma Sheet for a Microwave Agile Mirror Application," Bulletin of the American Physical Society 40, 1681 (1995).

12. K.L. Kelly, J.E. Scharer, W. Shen, M.H. Bettenhausen, N.T. Lam, B.G. Porter, "Microwave Reflections from a VUV Laser Produced Plasma Sheet," Bulletin of the American Physical Society 40, 1681 (1995).

13. J.E. Scharer, K. Kelly, G. Ding, W. Shen, M. Bettenhausen, N.T. Lam, and D. Synitsin, "VUV Laser Plasma Formation and Microwave Agile Mirror/Absorber," IEEE International Conference on Plasma Science, Boston June 3-5, Record 96CH35939, 188 (1996).

14. K.L. Kelly, J.E. Scharer, W. Shen, G. Ding, M.H. Bettenhausen, and N.T. Lam, "Microwave Reflections from a VUV Laser Produced Plasma Sheet," IEEE International Conference on Plasma Science, Boston June 3-5, Record 96CH35939, 261 (1996).

15. Yiannis Mouzouris, John E. Scharer, Mike Bettenhausen, "Wave Absorption Mechanisms and Transport for a Helicon Source Operation," Bulletin of the American Physical Society 41, 1473 (1996).

16. K.L. Kelly, J.E. Scharer, G. Ding, M. Bettenhausen, D. Sinitsyn, "Microwave Reflections from a VUV Laser Produced Plasma Sheet," Bulletin of the American Physical Society 41, 1602 (1996).

17. K.L. Kelly, J.E. Scharer, G. Ding, M.H. Bettenhausen, "Microwave Reflection from a VUV Laser Produced Plasma Sheet," IEEE International Conference on Plasma Science, San Diego May 19-22, Record 97CH36085, 134 (1997).

18. G. Ding, J.E. Scharer, K.L. Kelly, M.H. Bettenhausen, "Dynamics of a Laser Produced Plasma and its Properties for Microwave Reflection," IEEE

International Conference on Plasma Science, San Diego May 19-22, Record **97CH36085**, 133 (1997).

19. J.E. Scharer, K.L. Kelly, G. Ding, M.H. Bettenhausen, "VUV Laser Plasma Formation and Microwave Agile Mirror/Absorber," IEEE International Conference on Plasma Science, San Diego May 19-22, Record **97CH36085**, 153 (1997).

20. M.H. Bettenhausen, J.E. Scharer, Y. Mouzouris and K.L. Kelly, "Investigation of RF Effects on Laser Produced Plasmas," IEEE International Conference on Plasma Science, San Diego May 19-22, Record **97CH36085**, 202 (1997).

C.   Grant Modalities

During the past grant period, May 1, 1994 - August 31, 1997, the participants carrying out the research are as follows:

- John E. Scharer, Professor
- Dr. M. Bettenhausen, Postdoc (1996-97)
- Dr. W. Shen, Postdoc (1994-95),
- G. Ding, Graduate Student
- K. Kelly, Graduate Student
- Y. Mouzouris, Graduate Student (1994-95)
- S. Fusi, Minority Undergraduate Research Student (1995-96)
- A. Adjiwibawa, Undergraduate Research Student (1997)

29